

# Predictive Assessment on the Corrosion Consequences of Reinforced Concrete Frameworks Available Around Bhairahawa City Areas (Nepal) with Half-Cell Potential Measurement

Kamal Thapa Kunwar Magar<sup>1</sup>, Yuvraj Paudel<sup>1</sup>, Madhab Gautam<sup>1,2</sup>, Nootan Prasad Bhattarai<sup>1,\*</sup>, Jagadeesh Bhattarai<sup>1,\*</sup>

<sup>1</sup>Central Department of Chemistry, Tribhuvan University, Kirtipur 44618, Kathmandu, Nepal

<sup>2</sup>Department of Chemistry, Tribhuvan M. Campus, Tansen 32500, Palpa, Nepal

\*Email: neutan08@gmail.com; bhattarai\_05@yahoo.com

(Received: September 23, 2025, Received in revised form: November 21, 2025, Accepted: December 8, 2025, Available online: December 19, 2025)

DOI: <https://doi.org/10.3126/arj.v6i1.87528>

## Highlights

- Reinforced concrete frameworks, available in Bhairahawa city, Nepal, are studied
- Utilized half-cell potential to assess the corrosion risk of 34 RCFs
- The roofs of residential buildings and house pillars are at low risk of corrosion
- RCFs with rough/ cracked surfaces and moisture exposure are prone to corrosion
- Findings address the knowledge gap, design, & management of more resilient RCFs

## Abstract

A challenge to the long-term durability of reinforced concrete frameworks (RCFs) in urban areas is their corrosive degradation caused by their surrounding factors. This study examines the corrosion status of thirty-four reinforcing steel (RS) samples within the RCFs available in the Bhairahawa city areas of Nepal, using a simple, non-destructive, and in-situ electrochemical method of half-cell potential ( $E_{Hc}$ ) as per the ASTM C876-22b standards. This approach enables prediction of early corrosion activity in steel-reinforced concrete. Average half-cell potential values were used to classify corrosion probability zones as per ASTM C876-22b, i.e., low corrosion risk (LoCR) or less than 10% probability of corrosion, moderate corrosion risk (MoCR) or 10-90% probability of corrosion, and high corrosion risk (HiCR) or greater than 90% probability of corrosion. Results indicate that the RCFs categorized residential roofs and house pillars predominantly (i.e., two-thirds) fall within the LoCR category. Conversely, RCFs categorized within fencing pillars exhibit 66.7% HiCR and 33.3% MoCR. Most of the sewer pipes belonged to MCR, whereas most of the septic tanks are assumed to be LoCR. The study also identifies that structural elements with rough or cracked surfaces and prolonged exposure to moisture are particularly prone to RS within RCFs.

**Keywords:** concrete infrastructure, half-cell potential, reinforcing steel, reinforced concrete corrosion

## Introduction

One of the most widely used construction materials is concrete, valued for its high compressive strength and adaptability in design (Gragg, 2014). It can be shaped into various forms, allowing for creative and complex architectural designs. Its low tensile strength necessitates reinforcing steel rebar to enhance structural integrity in buildings, bridges, flyovers, and dams (Shunmuga

---

\*Corresponding author

Vembu & Ammasi, 2023). This unique combination of properties, along with its durability and relatively low cost, makes concrete a fundamental and versatile material in the construction industry (Li et al., 2022). Despite its widespread use, most of the reinforced concrete frameworks (RCFs) are susceptible to premature corrosive deterioration (Bhattacharjee, 2018). This electrochemical process is provoked by environmental factors such as moisture, chlorides, sulfates, and carbon dioxide (CO<sub>2</sub>), which lead to the premature failure of these infrastructures (Ali et al., 2024). A simple example of rust formation on the surface of a reinforcing steel within the concrete is an example of the RCFs corrosion (Bhattarai et al., 2021), in which the corrosiveness of the concrete enhances to corrode the steel, expanding its volume, leading to internal stress, cracking, and ultimately losing the structural durability, as illustrated in Fig. 1.

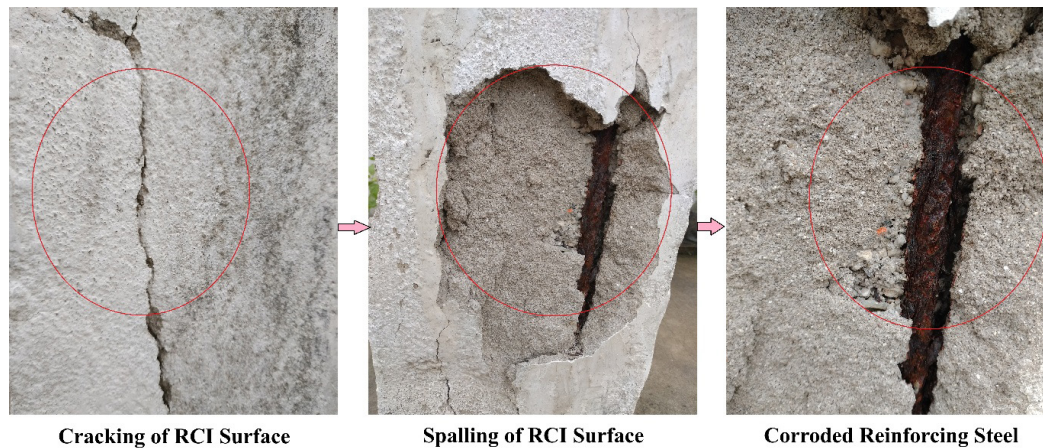


**Fig. 1.** The corrosion processes of a reinforcing steel within a reinforced concrete infrastructure (RCI).

Global production of concrete and mortar between 1990 and 2020 is fourfold, culminating in an estimated annual volume of approximately 26 gigatons in 2020 (Althoey et al., 2023). To meet the yearly demand for concrete, around four gigatons of cement were utilized during the same year (Watari et al., 2023). The effects of concrete corrosion on RCFs are minimized in the design phase, allowing for informed decisions to be made before construction, which in turn enables RCFs to survive for far longer (Kanagaraj et al., 2024). An examination optimizes and minimizes the maintenance time and costs. Reduced maintenance requirements can increase the asset's overall utilization and improve its environmental sustainability, which is crucial for increasing the longevity of the RCFs and economic benefits (Rusnak, 2025).

Many older RCFs in Nepal, constructed before the establishment of Nepal standard NBC 105:2020, lack adequate durability, making them highly vulnerable to corrosion-related damage (Shrestha et al., 2021). The corrosion process of the reinforcing steels begins with the oxidation of iron at anodic sites, followed by the flow of electrons to cathodic areas in the presence of environmental pollutant gases or ions with moisture. The resulting ferrous ions react with hydroxide ions, eventually forming expansive ferric oxide (rust), which causes the concrete to crack and spall, a sign of corrosion damage (Wang et al., 2024).

In this context, a non-destructive, in-situ electrochemical technique, half-cell potential ( $E_{HC}$ ) measurement, is used to monitor the corrosion conditions of the RCFs available at Bhairahawa city areas of Rupendehi district, Nepal. As outlined in the ASTM C876-22b (2022) standard, this technique provides a qualitative indication of corrosion or passivity activity and insight into the probability of concrete corrosion, helping to identify maintenance needs and areas for further investigation. While this technique is primarily qualitative, it is valuable for initial corrosion assessments (Yodsudjai & Pattarakittam, 2017).

The  $E_{HC}$  method is used to evaluate the likelihood of reinforcing steel corrosion in reinforced concrete structures using the ASTM C876-22b (2022) standard. It measures the electrical potential difference between reinforcement steel within RCFs and the reference electrode, adjusted on the concrete surface (Amiri et al., 2021). Although previous studies have assessed corrosion risks in certain regions of Nepal such as Kathmandu Valley (Phulara & Bhattarai, 2019), Pokhara Valley (Laudari et al., 2021), and the Butwal Sub-metropolitan area (Thapa Kunwar Magar et al., 2025), locations like Bhairahawa city areas remain insufficiently explored despite experiencing rapid urban growth and significant exposure of the environmental and the industrial pollutions.

This study employs the  $E_{HC}$  method to analyze the electrochemical potential values of steel in reinforced concrete structures across these cities, aiming to assess the severity, progression, and influencing factors of corrosion. The study seeks to develop

region-specific recommendations for structural maintenance and retrofitting. The findings are expected to address existing knowledge gaps and support the design and management of more resilient RCFs in Nepal.

## Materials and Methods

To predict the corrosion probability of reinforcing steel (RS) in thirty-four (34) RCFs, were investigated obeying purposive random sampling techniques, such as houses, pillars, sewer pipes, and septic tanks available in Bhairahawa city, including its central coordinates (27.5°N, 83.45°E), (Fig. 2), were meticulously assessed by recording their average  $E_{HC}$  values. After a careful visual investigation, the  $E_{HC}$  measurement method, as outlined in ASTM C876-22b (2022) criteria, was employed for this assessment. The  $E_{HC}$  measurement was performed within 10 days and temperature of outdoor climate and humidity were  $25 \pm 4^\circ\text{C}$  and humidity  $2 \pm 3\%$  respectively. Before recording the  $E_{HC}$  values of these concrete infrastructures, examination of their morphological and physical characteristics was painstakingly collected.

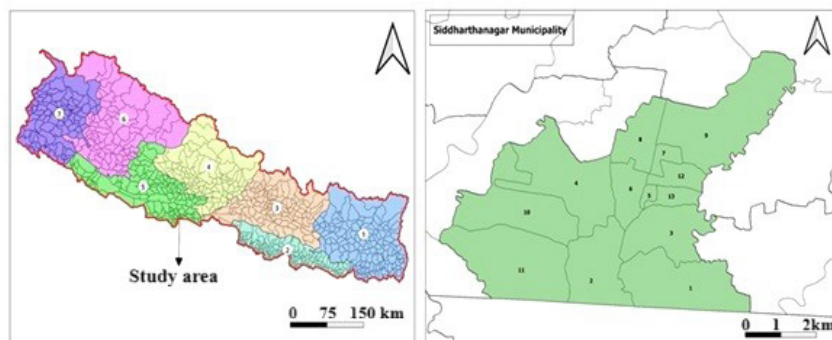


Fig. 2. Map for sampling sites of Bhairahawa city areas.

The arrangement for the  $E_{HC}$  measurement method of the ASTM C876-22b (2022) standard technique is as; the positive pole of the high-impedance multimeter should be attached to the reinforcing steel. The other negative pole of the multimeter needs to be connected to a reference electrode, i.e., either a saturated calomel electrode or a copper/copper sulfate electrode, which is inside a wetted sponge placed just above the surface of the RCFs, as demonstrated in Fig. 3.

The  $E_{HC}$  values measured can then be interpreted to assess the risk of reinforcing steel (RS) corrosion within the RCFs (Adriaman et al., 2022). If the reinforced concrete surface is too dry, it is essential to pre-wet the reinforced concrete structures in this technique (Laudari et al., 2021). Pre-wetting can be accomplished by spreading double-distilled water over the location to be tested or using a wet sponge for a fixed time before the  $E_{HC}$  measurement (Phulara & Bhattarai, 2019).

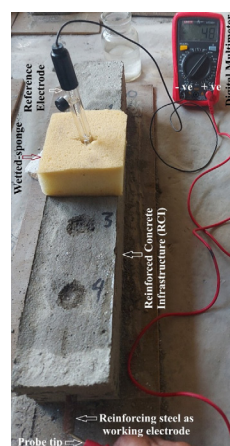


Fig. 3. Testing configuration for the measures of the half-cell potential ( $E_{HC}$ ) of the reinforcing steel within RCFs.

The half-cell potential ( $E_{HC}$ ) measurement approach was employed to qualitatively forecast the corrosion hazard of RS in reinforced concrete structures, aligning with the guidelines outlined in ASTM C876-22b (2022) protocol. This standard classifies

into three zones: a low corrosion risk (LoCR), with a probability of less than 10% likelihood of corrosion based on the average EHC value nobler than -126 mV (SCE), an uncertain or moderate corrosion risk (MoCR) value ranging from -126 mV to -276 mV, where a definitive conclusion of corrosion risk is not possible. Conversely, a value less than -276 mV signifies a high probability of corrosion risk (HiCR), exceeding a 90% likelihood of corrosion, as summarized in Table 1.

**Table 1.** Projection of three corrosion risk zones of the reinforcing steel in concrete infrastructures, established on the average  $E_{HC}$  value per ASTM C876-22b (2022) protocol.

$E_{HC}$ (mV vs SCE)	Corrosion Risk Zone	Corrosion Probability
More +ve than -126	Low corrosion risk (LoCR)	< 10% corrosion probability
Between -276 and -126	Moderate corrosion risk (MoCR)	10-90% corrosion probability
More -ve than -276	High corrosion risk (HiCR)	> 90% corrosion probability

An investigation was performed on the corrosion risk conditions of a total of 34 RCFs, using recorded  $E_{HC}$  values. Among these samples, fourteen house-roofs (RoHs), six house-pillars (PiHs), six fencing-pillars (PiFs), five sewer-pipes (SwPs), and three septic-tanks (SeTs) were selected using a purposive sampling procedure. First, the physical and morphological properties of these sample specimens, as well as the surrounding circumstances of the reinforced concrete infrastructure sampling sites, were documented before registering the experimental  $E_{HC}$  values *in situ*. The  $E_{HC}$  measurement was recorded using a digital multimeter (UNI-T model, Model No.: UT33D+, Hong Kong) under ASTM C876-22b (2022) protocol with a saturated calomel electrode (SCE) serving as the reference electrode and the exposed embedded reinforcing steel as the working electrode, as described elsewhere (Gautam et al., 2025). To ensure analytical consistency and enhance the reliability of the recorded values, four surface points (SurP) of each reinforced concrete sample were marked and monitored for their  $E_{HC}$  values, as illustrated in Fig. 3.

## Results and Discussion

The *in-situ* half-cell potential ( $E_{HC}$ ) measurement method was used to estimate the corrosion risk zone or the corrosion probability of the reinforced concrete infrastructures available in the Bhairahawa city. This study involved 34 samples from five categories: house roofs, house pillars, fancy pillars, sewer pipes, and septic tank walls, as in Tables 2, 3, and 4.

**Table 2.** Physical appearance and average  $E_{HC}$  values with standard deviation (n=4) of reinforced concrete roofs of house (RoH) exemplars available in Bhairahawa city areas.

S.N.	Sample Code	Physical Observations	$E_{HC}$ Values		Prediction of Corrosion Zone
			Average (n=4)	SD	
1	RoH-1	Old; rough and dry; no rust-stain on the surface; no cracking and spalling	-110.5	6.8	LoCR
2	RoH-2	Old; smooth and dry; rust-stain on the surface; no cracking and spalling	-155.5	4.4	MoCR
3	RoH-3	Old; smooth and dry; rust-stain on the surface; no cracking and spalling	-135.3	5.4	MoCR
4	RoH-4	Old; rough and dry; rust-stain on the surface; no cracking and spalling	-167.1	3.7	MoCR
5	RoH-5	Old; rough and dry; rust-stain on the surface; no cracking and spalling	-182.1	3.7	MoCR
6	RoH-6	Old; smooth and dry; rust-stain on the surface; no cracking and spalling	-174.5	7.6	MoCR
7	RoH-7	Old; rough and wet; no rust-stain on the surface; no cracking and spalling	-65.3	4.9	LoCR

8	RoH-8	Old; rough and dry; no rust-stain on the surface; no cracking and spalling	-39.1	3.3	LoCR
9	RoH-9	Old; rough and dry; no rust-stain on the surface; no cracking and spalling	-42.3	9.4	LoCR
10	RoH-10	Old; rough and dry; no rust-stain on the surface; no cracking and spalling	-62.8	9.5	LoCR
11	RoH-11	New; smooth and dry; no rust-stain on the surface; no cracking and spalling	-71.5	3.4	LoCR
12	RoH-12	New; rough and dry; no rust-stain on the surface; no cracking and spalling	-49.5	1.7	LoCR
13	RoH-13	Old; rough and dry; no rust-stain on the surface; no cracking and spalling	-94.1	2.6	LoCR
14	RoH-14	New; smooth and dry; no rust-stain on the surface; no cracking and spalling	-32.8	4.0	LoCR

It provides a comprehensive overview of the physical and morphological properties of the 34 RCFs exemplars, as well as their average  $E_{HC}$  values. To ensure consistent data collection, the monitored  $E_{HC}$  values were from four predefined surface points (SuP-1, SuP-2, SuP-3, and SuP-4) on each reinforced concrete structure. The average  $E_{HC}$  of the fourteen-house roof (RoH) samples (Table 2) revealed that most of these samples (nine samples, out of 14) are in the low corrosion risk zone (LoCR) or have less than 10% corrosion probability since the average  $E_{HC}$  values of these nine RoHs are in more noble than -126 mV (SCE), as summarized in Table 2. Only five RoH samples are assumed to be in the moderate corrosion risk (MoCR) zone with 10-90% corrosion probability. The outcomes disclosed that the house roofs with appearance of rust-stain on the surface, and a sign of fine cracking indicates the initiation of corrosion damage of reinforcing steel within the concreted roofs of the building structures, as proposed elsewhere (Loukil et al., 2024).

Similarly, six fencing-pillars (PiFs) and six house-pillars (PiHs), made of reinforced concrete, are investigated by recording the  $E_{HC}$  values to predict their corrosion probability. Only two fencing-pillars (PiF-1 & PiF-6) among six are susceptible to a high corrosion risk (HiCR) zone, or the corrosion probability is more than 90%. The remaining four PiFs are assumed to be in the moderate corrosion risk (MoCR) zone with 10-90% corrosion probability. However, most of the five tested PiHs, out of six, are in the low corrosion risk (LoCR) zone based on their recorded average  $E_{HC}$  values, which range between  $25.8 \pm 2.2$  and  $90.0 \pm 4.97$  mV (SCE), as summarized in Table 3.

**Table 3.** Physical appearance and average  $E_{HC}$  values with standard deviation ( $n=4$ ) for the prediction of corrosion for reinforced pillars of fencing (PiF) and pillars of house (PiH) exemplars available in Bhairahawa city areas.

S.N.	Sample Code	Physical Observations	$E_{HC}$ (mV vs SCE)		Prediction of Corrosion
			Average ( $n=4$ )	SD	
1	PiF-1	Old; rough (porous) and moist; rust-stain on the surface; cracking and spalling	-290.3	4.4	HiCR
2	PiF-2	Old; rough (porous) and dry; rust-stain on the surface; cracking and spalling	-185.8	2.2	MoCR
3	PiF-3	Old; rough (porous) and wet; rust-stain on the surface; cracking and spalling	-173.3	3.9	MoCR
4	PiF-4	Old; rough and moist; rust-stain on the surface; cracking and spalling	-180.1	6.2	MoCR
5	PiF-5	Old; rough (porous) and dry; rust-stain on the surface; cracking and spalling	-173.3	3.9	MoCR

6	PiF-6	Old; rough (porous) and moist; rust-stain on the surface; cracking and spalling	-286.0	5.3	HiCR
7	PiH-1	Old; smooth and moist; rust-stain on the surface; no cracking and spalling	-134.8	3.3	MoCR
8	PiH-2	New; smooth and dry; rust-stain on the surface; no cracking and spalling	-34.0	2.6	LoCR
9	PiH-3	Old; smooth and dry; no rust-stain on the surface; no cracking and spalling	-47.3	2.9	LoCR
10	PiH-4	Newly constructing; smooth and dry; no rust-stain on the surface; no cracking and spalling	-25.8	2.2	LoCR
11	PiH-5	New; smooth and dry; no rust-stain on the surface; no cracking and spalling	-34.1	2.6	LoCR
12	PiH-6	Old; smooth and dry; no rust-stain on the surface; no cracking and spalling	-93.0	4.9	LoCR

The analysis revealed that the fencing pillars are more susceptible to corrosion compared to the house pillars. This increased vulnerability is primarily due to visible rust stains on the surface, as well as issues like cracking and spalling. Additionally, the fencing concrete pillars are more exposed to corrosive environmental agents than the internal house pillars, contributing to their higher risk of corrosion (Dimova et al., 2024). Similarly, out of 8 city sewer pipes (SwPs) and septic tanks (SeTs), only one SeT (i.e., SeT-2) is prone to a high corrosion risk (HiCR) zone, since the average  $E_{HC}$  of SeT-2 is more negative than -276 mV vs SCE, i.e.,  $-283.8 \pm 4.99$ , although the remaining two septic tank walls are assumed to be in a low corrosion risk (LoCR) zone, recording the  $E_{HC}$  values between  $-52.8 \pm 3.09$  and  $-76.5 \pm 4.19$ , as illustrated in Table 4. According to Table 4, 80% of the five sewer pipe samples are in a moderately corrosion risk (MoCR) zone, except SwP-4. Research indicates that the conversion of hydrogen sulfide, one of the aggressive chemicals in the sewer, into sulfuric acid is a major contributor to the decay of reinforced concrete in sewer environments. This process not only affects the concrete itself but also impacts surrounding factors and the composition of the sewage (Pramanik et al., 2024).

**Table 4.** Physical appearance and average  $E_{HC}$  values with standard deviation (n=4) for the prediction of corrosion for reinforced sewer pipe (SwP) and septic tank (SeT) exemplars available in Bhairahawa city areas.

S.N.	Sample		$E_{HC}$ (mV vs SCE)		Prediction of Corrosion
	Code	Physical Observation	Average (n=4)	SD	
1	SwP-1	Old; rough and moist; rust-stain on the surface; cracking and spalling	-162.0	4.2	MoCR
2	SwP-2	Old; rough (porous) and moist; rust-stain on the surface; cracking and spalling	-226.5	3.4	MoCR
3	SwP-3	Old; rough (porous) and dry; rust-stain on the surface; cracking and spalling	-144.0	2.6	MoCR
4	SwP-4	Old; rough (porous) and dry; rust-stain on the surface; no cracking and spalling	-117.5	3.0	LoCR
5	SwP-5	Old; rough (porous) and moist; rust-stain on the surface; cracking and spalling	-153.8	2.9	MoCR
6	SeT-1	New; smooth and dry; no rust-stain on the surface; no cracking and spalling	-76.5	4.2	LoCR
7	SeT-2	Old; rough (porous) and moist; rust-stain on the surface; cracking and spalling	-283.8	4.9	HiCR
8	SeT-3	Old; rough and moist; rust-stain on the surface; no cracking and spalling	-52.8	3.1	LoCR

The average  $E_{HC}$  data and error bar of the standard deviation, tabulated in Tables 2-4, are graphically presented in Figs. 4, 5, and 6 for the house roofs, building & fancy pillars, and sewer pipes with septic tanks' wall, respectively. These results clearly demonstrated that the standard error bars of all the 34 RCFs, belonging to five groups (i.e., RoH, PiH, PiF, SwP, and SeT), are within the range of 10 mV (SCE), indicating the occurrence of three degrees of corrosion (i.e., LoCR, MoCR, and HiCR) under the uniform or general class of corrosion, not of localized corrosion (Sawada et al., 2025), because all the sampling areas are assumed to be heavily polluted by industrial pollutants.

These consequences are outlined in the pie diagrams, as depicted in Fig. 7. Out of the fourteen-house roofs (RoHs), 64.3% of the representative samples are considered secure, with a less than 10% probability of corrosion risk, and the remaining 35.7% of the RoHs are in a moderate corrosion probability zone [Fig. 7(a)]. In this investigation, among the six examined fencing pillars (PiFs), 66.3% are in moderate corrosion risk (MoCR) zones, while 33.7% are in high corrosion risk (HiCR) zones, as shown in Fig. 7(b). In the same way, the pie chart demonstrated that 83.3%, 20%, and 66.7% RCFs of PiH, SwP, and SeT are classified as low corrosion risk (LoCR) zone among the six pillars of house (HoPs), five sewer pipes (SwP), and three walls of the septic tank (SaTs), as displayed in Figs. 7(c), 7(d), and 7(e), respectively.

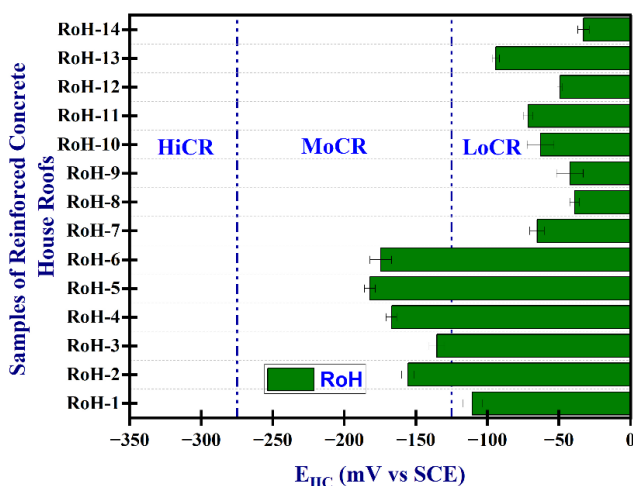


Fig. 4. Average  $E_{HC}$  with error bar showing the corrosion risk zone of the reinforced concrete roof samples of house.

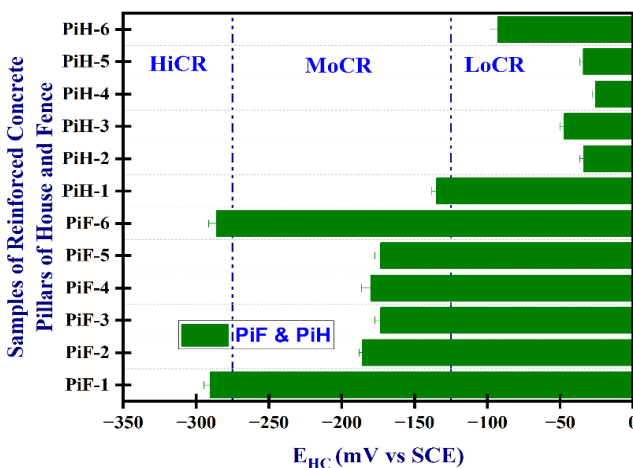


Fig. 5. Average  $E_{HC}$  with error bar showing the corrosion risk zone of the investigated reinforced concrete pillar samples of house and fence.

Consequently, the analyzed  $E_{HC}$  data reveal that 33.3% of the fencing pillars and 33.3% of the septic tank walls are the most corrosion-prone reinforced concrete items examined in this study, which focused on the Bhairahawa city area. This assessment included six fencing pillars and four septic tank walls. In contrast, the residential building components (i.e., roofs and pillars) demonstrate a remarkably high degree of durability and hence, a very low degree of corrosion risk. These findings are consistent with the results of previous studies by Phulara & Bhattarai (2019), Laudari et al. (2021), and Thapa Kunwar Magar et al. (2025),

who similarly assessed the durability characteristics of reinforced concrete structures of the Kathmandu Metropolitan, Pokhara Metropolitan, and Butwal Sub-metropolitan areas of Nepal using corrosion potential mapping methods. This previous research, including the present study, concludes that the  $E_{HC}$  approach seems to be effective in predicting structural integrity and evaluating potential corrosion risks.

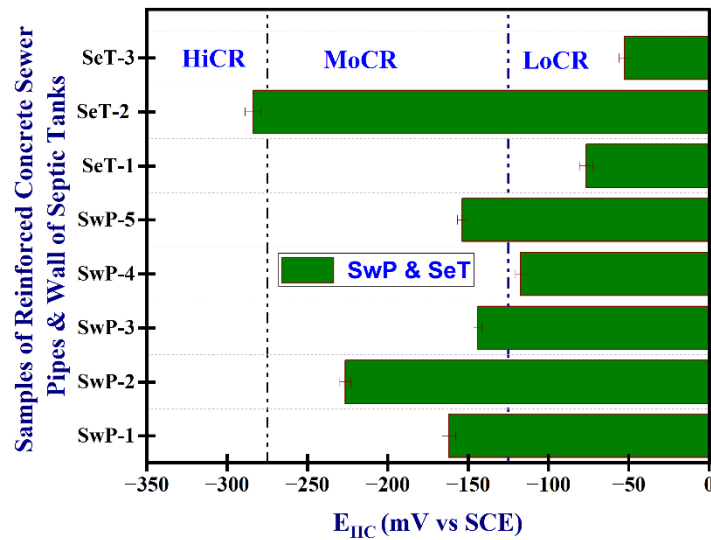


Fig. 6. Average  $E_{HC}$  with error bar showing the corrosion risk zone of the investigated reinforced concrete sewer pipes and wall of septic tanks.

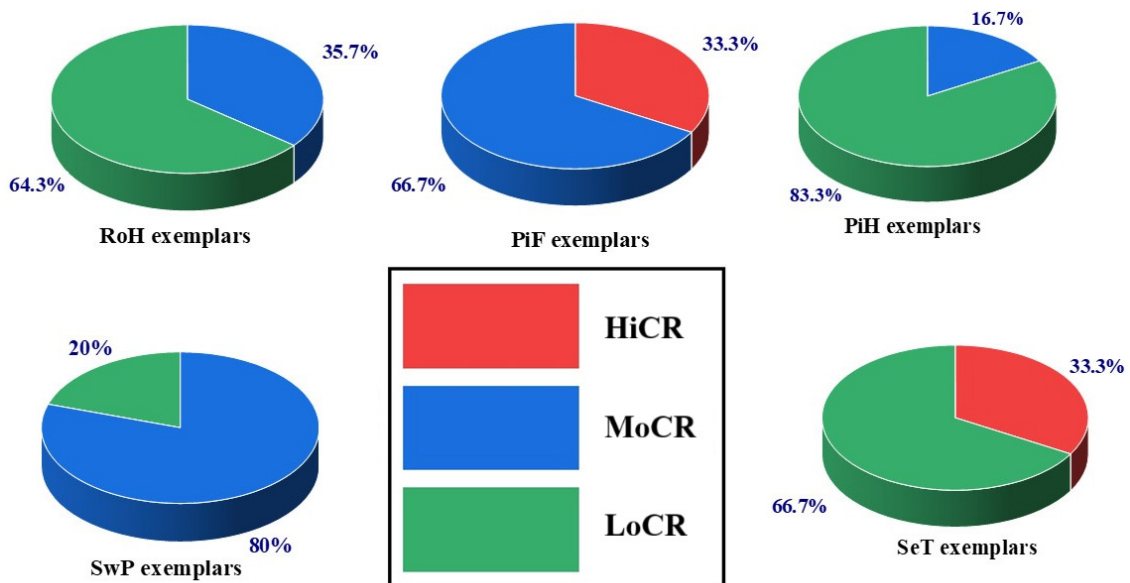


Fig. 7. Pie charts showing three different corrosion probabilities of varieties of the reinforced concrete infrastructures available in Bhairahawa city areas of Nepal.

## Conclusions

The study identified the corrosion state of the thirty-four (34) reinforced concrete infrastructures available in Bhairahawa city areas of Nepal, using the *in-situ* half-cell potential ( $E_{HC}$ ) measurement procedure aligned with ASTM C876-22b (2022) protocols. Most of the house roofs, building pillars, and walls of septic tanks, sampled from the study areas, are found to be comparatively durable, showing few signs of corrosion. The roofs and pillars are crucial components of buildings, highlighting the importance of regular inspections and maintenance.



In contrast, approximately one-third of the fencing pillars and walls of the septic tanks of the study areas are particularly susceptible to corrosion, with many exhibiting a high to moderate risk. This situation indicates that these concrete facilities in the areas require immediate attention to apply appropriate corrosion preventive techniques. Septic tanks and sewer pipes also exhibit significant and moderate corrosion risks, respectively. The investigation highlights that sampled RCFs exhibiting perceptible cracks, signs of delamination, and exposure to dampness are more susceptible to reinforcing steel corrosion within the varieties of concrete infrastructures. Therefore, preventive maintenance is recommended for RCFs with EHC < -276 mV.

## Author contributions

JB, NPB & MG planned experimentations; experimental works, and data examination by KTKM, YRP, and MG; analyzed the data and results summarization by MG, NPB, and JB; prepared the manuscript draft by MG and KTKM, and did the final corrections by JB and NPB. All authors read and authorized the final manuscript.

## Conflict of interest

The authors assert that they have no contending interests.

## Data availability statement

Upon request, the corresponding authors will supply supplementary data.

## References

- Gagg, C.R. (2014). Cement and concrete as an engineering material: an historic appraisal and case study analysis. *Engineering Failure Analysis*, 40, 114-140. DOI: <http://dx.doi.org/10.1016/j.engfailanal.2014.02.004>
- Shunmuga Vembu, P.R., & Ammasi, A.K. (2023). A comprehensive review on the factors affecting bond strength in concrete. *Buildings*, 13(3), 577. DOI: <https://doi.org/10.3390/buildings13030577>
- Li, Z., Yoon, J., Zhang, R., Rajabipour, F., Srubar III, W.V., Dabo, I., & Radlinska, A. (2022). Machine learning in concrete science: applications, challenges, and best practices. *Npj Computational Materials*, 8, 127. DOI: <https://doi.org/10.1038/s41524-022-00810-x>
- Bhattacharjee, J. (2018). Deterioration of concrete structures along with case studies in India. *Proceedings of the Institution of Civil Engineers-Forensic Engineering*, 171(2), 80-90. DOI: <https://doi.org/10.1680/jfoen.17.00010>
- Ali, M., Shams, M.A., Bheel, N., Almaliki, A.H., Mahmoud, A.S., Dodo, Y.A., & Benjeddou, O. (2024). A review on chloride induced corrosion in reinforced concrete structures: lab and *in-situ* investigation. *RSC Advances*, 14(50), 37252-37271. DOI: <https://doi.org/10.1039/d4ra05506c>
- Bhattarai J., Somai M., Acharya N., Giri A., Roka A., & Phulara N.R. (2021). Study on the effects of green-based plant extracts and waterproofers as anti-corrosion agents for steel-reinforced concrete slabs. *E3S Web of Conferences*, 302, 02018. DOI: <https://doi.org/10.1051/e3sconf/202130202018>
- Althoey, F., Ansari, W.S., Sufian, M., & Deifalla, A.F. (2023). Advancements in low-carbon concrete as a construction material for the sustainable built environment. *Developments in the Built Environment*, 16, 100284. DOI: <https://doi.org/10.1016/j.dibe.2023.100284>
- Watari, T., Cao, Z., Serrenho, A.C., & J. Cullen, J. (2023). Growing role of concrete in sand and climate crises. *iScience*, 26(5), 106782. DOI: <https://doi.org/10.1016/j.isci.2023.106782>.
- Kanagaraj, B., Priyanka, R., Anand, N., Kiran, T., Andrushia, A.D., & Lubloy, E. (2024). A sustainable solution for mitigating environmental corrosion in the construction sector and its socio-economic concern. *Case Studies in Construction Materials*, 20, e03089. DOI: <https://doi.org/10.1016/j.cscm.2024.e03089>
- Rusnak, C.R. (2025). Sustainable strategies for concrete infrastructure preservation: a comprehensive review and perspective. *Infrastructures*, 10(4), 99. DOI: <https://doi.org/10.3390/infrastructures10040099>

- Shrestha, J., Lamichhane, A., Giri, B., Koirala, B.R., & Paudel, N. (2021). Impact of revised code NBC105 on assessment and design of low rise reinforced concrete buildings in Nepal. *Journal of the Institute of Engineering*, 16(1), 1-5. DOI: <http://dx.doi.org/10.3126/jie.v16i1.36527>
- Wang, Q., Wang, Z., Li, C., Qiao, X., Guan, H., Zhou, Z., & Song, D. (2024). Research progress in corrosion behavior and anti-corrosion methods of steel rebar in concrete. *Metals*, 14(8), 862. DOI: <https://doi.org/10.3390/met14080862>
- ASTM C876-22b. (2022). Standard test Method for Corrosion Potentials of Uncoated Reinforcing Steel in Concrete. In annual book of ASTM standards, *ASTM International*, West Conshohocken, PA, USA. DOI: <https://doi.org/10.1520/C087615>.
- Yodsudjai, W., & Pattarakittam, T. (2017). Factors influencing half-cell potential measurement and its relationship with corrosion level. *Measurement: Journal of the International Measurement Confederation*, 104, 159-168. DOI: <https://doi.org/10.1016/j.measurement.2017.03.027>
- Amiri, A.S., Erdogmus, E., & Richter-Egger, D. (2021). A comparison between ultrasonic guided wave leakage and half-cell potential methods in detection of corrosion in reinforced concrete decks. *Signals*, 2, 413-433. DOI: <https://doi.org/10.3390/signals2030026>
- Phulara, N.R., & Bhattarai, J. (2019). Assessment on corrosion damage of steel-reinforced concrete structures of Kathmandu valley using corrosion potential mapping method. *Journal of the Institute of Engineering*, 15(2), 47-56. DOI: <https://doi.org/10.3126/jie.v15i2.27640>.
- Laudari, I., Phulara, N.R., Gautam, M., & Bhattarai, J. (2021). Evaluation of Corrosion Condition of Some Steel-Reinforced Concrete Infrastructures Available in Pokhara Valley of Nepal. *Tribhuvan University Journal*, 36(01), 1-17. DOI: <http://dx.doi.org/10.3126/tuj.v36i01.43509>.
- Thapa Kunwar Magar, K., Paudel, Y., Gautam, M., Bhattarai, N.P., & Bhattarai, J.B. (2025). Durability judgment of reinforced concrete infrastructures around Butwal sub-metropolitan city areas with corrosion potential mapping method. *Journal of Nepal Chemical Society*, 45(2), 147-156. DOI: <http://dx.doi.org/10.3126/jncs.v45i2.83064>.
- Adriman, R., Bin M. Ibrahim, I., Huzni, S., Fonna, S., & Ariffin, A. K. (2022). Improving half-cell potential survey through computational inverse analysis for quantitative corrosion profiling. *Case Studies in Construction Materials*, 16, e00854. DOI: <https://doi.org/10.1016/j.cscm.2021.e00854>
- Gautam, M., Subedi, D.B., Dhungana, J.R., Bhattarai, N.P., & Bhattarai, J. (2025). Utilization of bark extract of *Phyllanthus emblica* as a sustainable corrosion inhibitor to reinforced concrete Infrastructures in Aggressive Environments. *E3S Web of Conferences*, 610, 03002. DOI: <http://dx.doi.org/10.1051/e3sconf/202561003002>
- Loukil, O., Adelaide, L., Bouteiller, V., Quiertant, M., Ragueneau, F., & Chaussadent, T. (2024). Investigation of corrosion product distribution and induced cracking patterns in reinforced concrete using accelerated corrosion testing. *Applied Sciences*, 14(23), 11453. DOI: <https://doi.org/10.3390/app142311453>
- Dimova, S., Lopez, C.S.P., Sousa, M.L., Rianna, G., Bastidas-Arteaga, E., Nogal, M., Gervásio, H., Martorana, E., Reder, A., & Athanasopoulou, A. (2024). Impact of climate change on the corrosion of the European reinforced concrete building stock. Joint Research Centre, Hal-04543682. DOI: <https://hal.science/hal-04543682v1>
- Pramanik, S.K., Bhuiyan, M., Robert, D., Roychand, R., Gao, L., Cole, I., & Pramanik, B.K. (2024). Bio-corrosion in concrete sewer systems: mechanisms and mitigation strategies. *Science of the Total Environment*, 921, 171231. DOI: <https://doi.org/10.1016/j.scitotenv.2024.171231>
- Sawada, K., Okazaki, S., Inaba, T., Sakuma, M., & Azuma, K. (2025). Evaluation of corrosion potential stability of stainless steels in dilute electrolyte solution for application to a quasi-reference electrode used in electrochemical sensing system. *Chemosensors*, 13(1), 4. DOI: <https://doi.org/10.3390/chemosensors13010004>